Turkish Journal of Electrical Engineering & Computer Sciences

http://journals.tubitak.gov.tr/elektrik/

Research Article

Turk J Elec Eng & Comp Sci
(2018) 26: 1056 – 1068

doi:10.3906/elk-1702-58

Prediction of the mass unbalance of a variable speed induction motor by stator current multiple approaches

Abdelkarim BOURAS*, Slimane BOURAS, Samir KERFALI
Electromechanical Systems Laboratory, Department of Electromechanical, Badji Mokhtar – Annaba University, Annaba, Algeria

Received: 04.02.2017 • **Accepted/Published Online:** 14.11.2017 • **Final Version:** 30.03.2018

Abstract: Generally, rotor mass unbalance is one of the most probable causes of the majority of degradations suffered by electric drives in an industrial environment (current pumping, rolling problem, misalignment, etc.), especially those with high power and variable speed. This document is an experimental contribution to the reliable detection of mass unbalance and changes in its severity if, by necessity of service, the system is subjected to a speed variation. The implementation of the technical orbits Park, strengthened by the application of the Fourier transforms (FFT, STFT) to the Park vector of the stator current allowed the identification of the unbalance defect at low frequency. The sequence of current analytical approaches favors the convergence towards an unambiguous reading of the mass unbalance defect. A comparative table has been drawn up in order to observe the evolution of the gravity of this mechanical defect in the case of a speed variation of the induction motor. The results obtained by this multifaceted approach are very satisfying and can contribute to a self-diagnostic with the assistance of a decision-making technique.

Key words: Induction motors, current stator, fault detection, Fourier transforms, orbits

1. Introduction

Since the advent of electronic frequency inverters, induction motors have replaced many industrial applications using DC motors. Among the damage suffered by the induction motor in electromechanical drives, unbalance occupies an important place in industry, especially for high power and variable speeds. This mechanical defect can be cited as the cause of the majority of breakdowns and has very critical material and financial consequences. Pumping the resulting current is responsible for the disconnection of the electronic components of the speed variator and the degradation of the elements ensuring the mechanical transmission (bearing, clutch, gearing, etc.). Therefore, early diagnosis of any unbalance affecting electromechanical motor systems based on induction becomes imperative. In recent decades, research has favored the spectral analysis of stator current to obtain information on the predictive detection of mechanical defects, to the detriment of the vibratory and acoustic signal [1,2]. Motor current signature analysis (MCSA) has obtained many research results in the diagnosis of electrical degradations (breakdown of bars, etc.) and mechanical degradations (bearings, gears, etc.) suffered by electric drives [3–5]. This experimental work aims to exploit different consecutive signatures in order to converge towards an accurate reading of the unbalance fault, which can be masked by other defects in low frequencies. The application of the Park orbit only indicates the presence of an anomaly, while the introduction of the various Fourier transforms of the current of the three phases and components of the Park vector of stator

*Correspondence: karim.bouras@hotmail.com

current role sheds light on the nature of the defect [6–9]. Furthermore, this paper discusses the impact of speed variation when the engine is experiencing a mechanical unbalance and experimentally deduces its degree of severity.

2. Transfer of mechanical damage to the stator current

Mechanical defects external to the motor, or related to the load, cause oscillations of the load torque [10–13]. The induction motor acts here as a sensor for torque oscillation detection. In the presence of an oscillating torque, the distribution of the surface current, which is sinusoidal for an ideal machine, will be modulated in phase $\mathrm{i}_{to}\ (t)$ for an arbitrary phase:

$$i_{t0}\,(t) = i_s\,(t) + i_r\,(t) = i_s \sin\left(\omega_s t\right) + i_r \sin\left(\omega_s t + m\cos\left(\omega_c t - \emptyset_a\right) - \emptyset_r\right), \tag{1}$$

where $\emptyset_a$ denotes the phase angle of the modulation.

The detection and the thorough analysis of the instantaneous stator current of the induction motor will be very significant for the diagnosis of the unbalance affecting the electric actuator [14–17].

3. Unbalance signatures by various current analytical approaches

3.1. Diagnostic approach through the Park orbits

The components (i_{ds} and i_{qs}) of the Park vector in reference axes linked to the rotor can be expressed according to the supply phasic currents (i_a, i_b, i_c) of the induction motor by

$$\begin{cases} i_a = i_m \sin\left(\omega t - \varphi\right) \\ i_b = i_m \sin\left(\omega t - \frac{2\pi}{3} - \varphi\right) \\ i_c = i_m \sin\left(\omega t - \frac{4\pi}{3} - \varphi\right) \end{cases}, \tag{2}$$

where
i_a, i_b, and i_c: the three stator currents
i_m: the maximum value of the supply phase current
ω: the supply frequency
φ: the phase angle
t: the time variable.

The components of the Park vector are expressed as

$$i_d = \sqrt{\frac{2}{3}} i_a - \frac{1}{\sqrt{6}} i_b - \frac{1}{\sqrt{6}} i_c, \tag{3}$$

$$i_q = \frac{1}{\sqrt{2}} i_b - \frac{1}{\sqrt{2}} i_c. \tag{4}$$

Under ideal engine manufacturing and functioning conditions, the components of the Park vector for the stator current can be expressed as follows:

$$i_d = \frac{\sqrt{6}}{2} i \sin \omega_s t, \tag{5}$$

$$i_q = \frac{\sqrt{6}}{2} i \sin(\omega_s t - \pi/2), \tag{6}$$

where
i: maximum current value of phase current
ω_s : frequency
t: variable time.

In the 3D stator current pattern, a circle centered at the origin of the coordinates is denoted for ideal condition, where its radius R is

$$R^2 = i_a^2 + i_b^2 + i_c^2. \tag{7}$$

The technique of approach of park vector makes it possible to detect and to locate defects. Figure 1 shows that when the engine is in nondegraded operation (healthy motor), the module of Park vector of the current is generally constant and, consequently, the corresponding representation is a circle centered at the origin of the reference axes (d, q). However, if the engine is affected by an anomaly of any kind, then the equations are no longer valid and an ellipsoid is obtained. The degree of deformation of the orbit, represented by the radius ratio, indicates the severity of the dysfunction [18–21]. However, the approach of the Park vector does not take into account the nonideality of the electrical machines and the unbalances of the supply voltages. It is difficult to isolate the various defects using only this method, knowing that many failures may cause a similar deviation of the current.

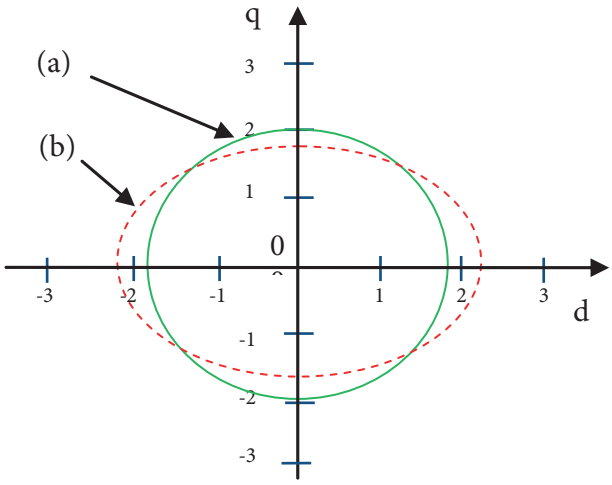

Figure 1. Orbit Park: normal engine (a) and degraded motor (b).

3.2. The FFT approach

Many signal processing tools are used to characterize the origins of defects from the spectra. The Fourier transform (FFT) [22] is well suited to analyze the stationary phenomena. The component at the frequency f of a time signal $x(t)$ is expressed by

$$X(f) = \int_{-\infty}^{+\infty} x(t)\, e^{-j2\pi ft}. \tag{8}$$

In order to better understand the nature of the failure, we introduce the frequency signatures successively via spectral analysis of the three feed currents (i_a, i_b, i_c) of the induction motor and the components of the Park vector of the current (extended Park vector analysis, EPVA).

$$i_p = i_{ds} + j i_{qs}, \tag{9}$$

$$\begin{cases} i_{ds} = \sqrt{\frac{2}{3}}[i_a \cos\theta + i_b \cos\left(\theta - \frac{2\pi}{3}\right) + i_c \cos\left(\theta - \frac{4\pi}{3}\right)] \\ i_{qs} = \sqrt{\frac{2}{3}}[i_a \sin\theta + i_b \sin\left(\theta - \frac{2\pi}{3}\right) + i_c \sin\left(\theta - \frac{4\pi}{3}\right)] \end{cases}. \tag{10}$$

This technique is based on the use of spectral analysis of the oscillatory component of the Park vector module of the stator current [23] to detect the presence of anomalies affecting the engine. The level of information provided by this technique, which takes into account the three currents in the three stator phases, is greater than that of a single phase. It offers a more meaningful spectrum than the one obtained by the conventional spectral analysis of the motor. The unbalance causes the appearance of harmonics in the spectra of current signals. The application of Fourier analysis over several periods of continuous operation of the machine shows two peaks at the frequencies ($f_s \pm 1 \times f_r$) and thus allows extracting the exact information about the presence of the mass unbalance.

3.3. Application of short-term Fourier transform to the Park vector

The short-time Fourier transform (STFT), also known as the sliding window Fourier transform, provides maps of a two-dimensional signal (time–frequency). The idea is to analyze the signal window by window [24–26]. The Fourier transform of each windowed signal portion is calculated as follows:

$$STFT_x^w(\tau, \mathrm{f}) = \int_t \mathrm{x}(t) \cdot w^*(t-\tau) \cdot e^{-j2\pi t f} dt, \tag{11}$$

where

$x(t)$: represents the sampled time signal.

w(t): the time window of width T and centered at τ which allows extracting a portion of signal.

$w*$: denotes the conjugate complex of w.

The application of STFT to the Park vector of the stator current is simpler and offers more for the confirmation of the nature of degradation.

4. Experimental set up

The experimental work is split into two test campaigns. The first test campaign focused on an engine in sound condition, whose characteristics are shown in Table 1. The frequency at the output of the speed variator (Altivar ATV12, 0.75 kW, 1 HP, 200/240 V; Schneider Electronics, Rueil-Malmaison, France) was set at 50 Hz and subsequently reduced to 35 Hz and 25 Hz in order to reduce the engine speed. The oscilloscope is connected to the current sensor (Chauvin Arnoux caliber 0.01–10 A and type: PAC 12; Paris, France).

The acquisition of the currents was made by a digital oscilloscope HAMEG507 equipped with software SP107 E. This device allows the acquisition of the signal on 8 bits with a sampling frequency between 1 kHz and 2.5 MHz. The measured current data were uploaded to a PC. The representation of the different spectra was obtained using programs written in the MATLAB environment.

Table 1. Rated parameters of the tested machine.

Power	Frequency	Voltage (Δ/Υ)	Current (Δ/Υ)	Speed	Pole pair (2 p)
270 W	50 Hz	220/380 V	1.43/0.80 A	1400 rpm	4

The second series of tests concerned the operation of the engine with an artificial unbalance made by fixing a mass of 50 g to a disk placed on the rotor shaft of the engine. The artificial fault produced characteristic fault frequencies. The latter allowed us to study the impact and the negative effect of the presence of the unbalance defect on the variable-speed induction motor. Figure 2 presents the test bench and the experimental configuration of the proposed approach for on-line induction motor fault detection and diagnosis.

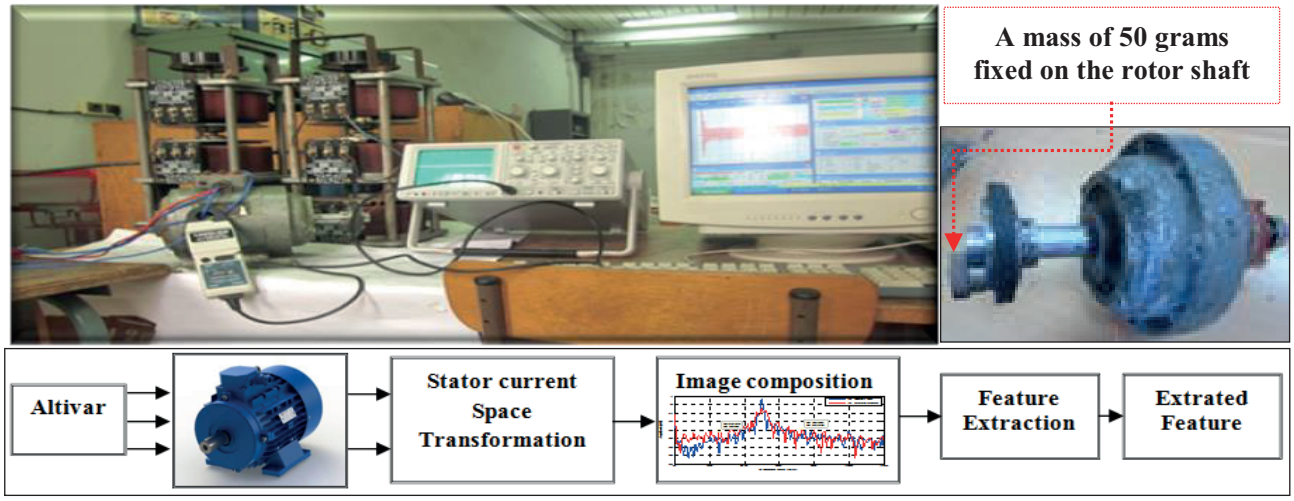

Figure 2. Experimental set up.

5. Experimental results of the approaches proposed for the predictive detection of unbalance defect

5.1. Application of Park orbit

Figure 3 shows the orbit obtained by applying the Park technique to the Park vector of the stator current when motor is operating in nondegraded mode (Healthy). The representation obtained is an ellipse close in shape to a circle.

An artificial unbalance on the motor caused a deformation of the orbit with a thickening of its contour (Figure 4). This indicates the presence of degradation at the level of the motor. However, the problem is that the Park technique cannot provide a concrete idea either of the nature of the defect or its exact location. Therefore, to expose the defect affecting the engine, it is necessary to enhance the Park (3D) approach with Fourier transforms. Although spectral analysis using FFT is conventional, the results obtained are very competitive in the field of mechanical fault detection.

5.2. Application of the FFT to phasic currents i_a, i_b, and i_c

The characteristic frequency of the unbalance defect is present on each side of the fundamental at 50 Hz. These results are in accordance with what was obtained in the theoretical context concerning the unbalance:

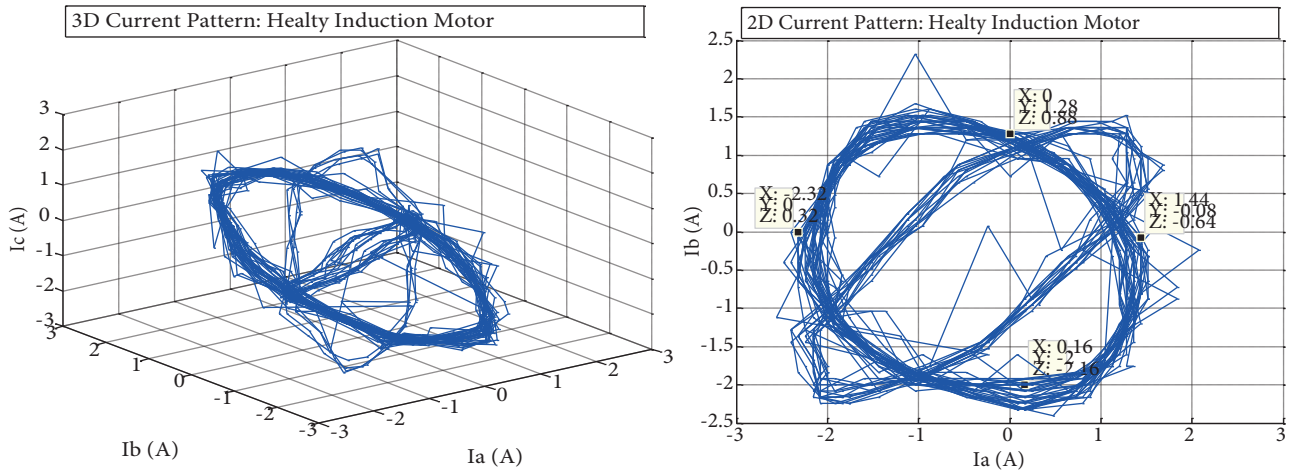

Figure 3. Stator current pattern for a healthy motor: 3D and orthogonal view.

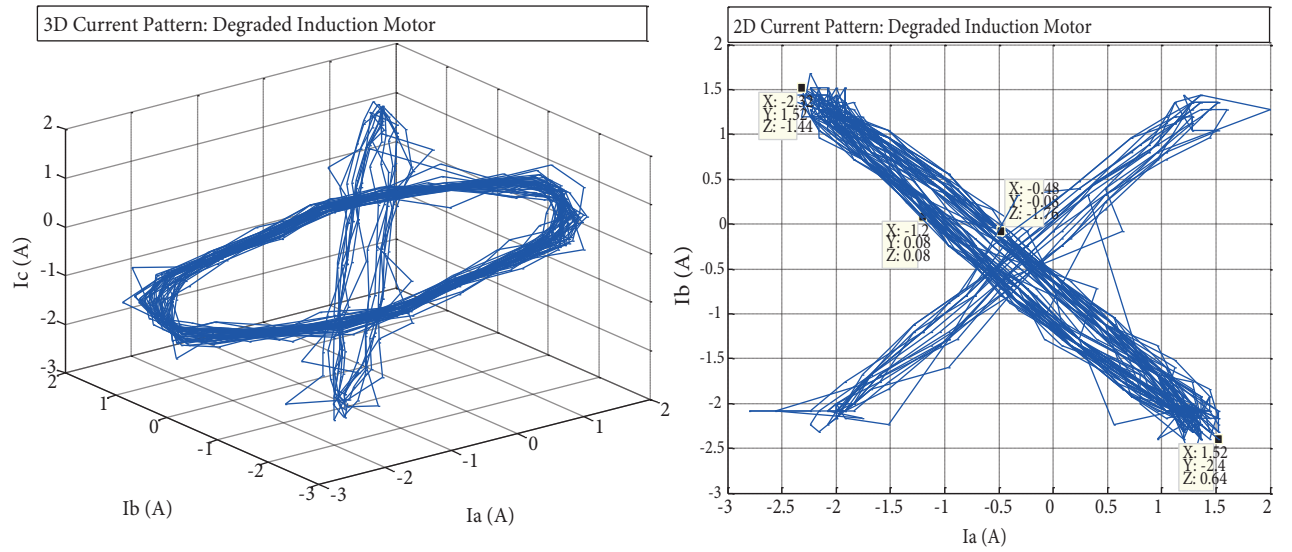

Figure 4. Stator current patterns for a motor with an unbalance fault: 3D and orthogonal view.

$$f_{unb} = f_s \pm (1 \times f_r), \tag{12}$$

$$f_r = n_{rot}/60 \tag{13}$$

The measured speed at no-load motor is $n_{rot} = 1470$ rpm for $f = 50$ Hz, $f_{r\max} = 1470 / 60 = 24.50$ Hz, and $f_{r\min} = 0.9 \times (1470 / 60) = 22.05$ Hz.

The line around the fundamental $f = 50$ Hz, which has the greatest amplitude in the frequency ranges below, is then searched on the spectrum of the current:

$f_{unb\min} = f_s - f_{r\min} = 27.95$ Hz, and $f_{unb\max} = f_s + f_{r\min} = 72.05$ Hz.

$f_{unb\min} = f_s - f_{r\max} = 25.50$ Hz, and $f_{unb\max} = f_s + f_{r\max} = 74.50$ Hz.

$f_{unb\min} = [25.50$ Hz, 27.95 Hz$]$, and $f_{unb\max} = [72.05$ Hz, 74.50 Hz$]$.

Figures 5a–5c present the stator current spectra of the currents of the three phases i_a, i_b and i_c, respectively, in a healthy engine (blue line) and in one with mass unbalance (red line). Table 2 summarizes the results expressed by the characteristic frequencies of the imbalance defect around the fundamental $f = 50$ Hz and their respective amplitudes.

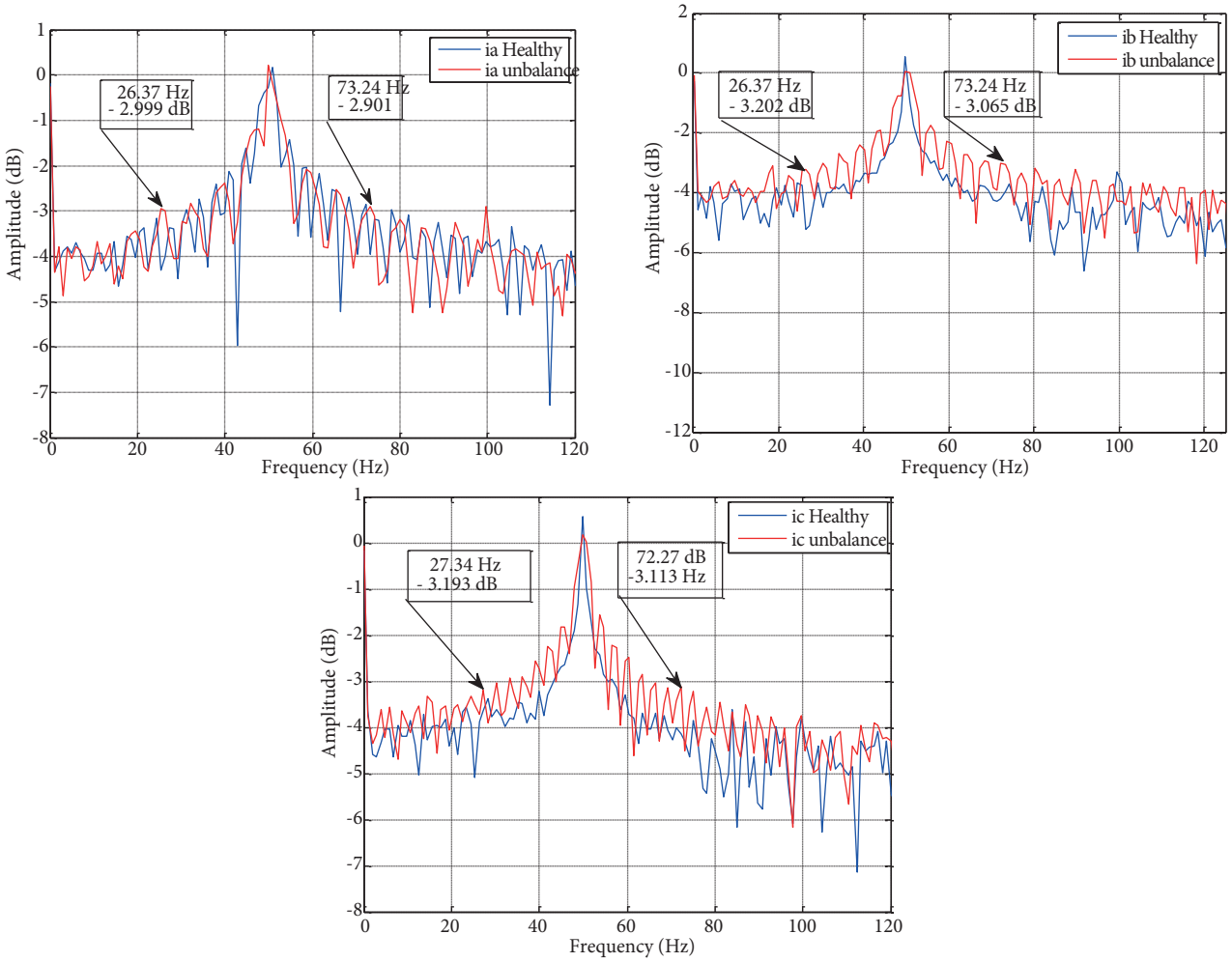

Figure 5. a) Spectrum of the current of phase A, healthy and degraded induction motor. b) Spectrum of the current of phase B, healthy and degraded induction motor. c) Spectrum of the current of phase C, healthy and degraded induction motor.

5.3. Application of the FFT to the Park vector of the stator current

Performing a spectral analysis of the stator current for each phase becomes a bit tedious; however, it is possible to make this approach to the FFT simpler by applying it only to the Park vector representing the current. It has been shown in several studies that the Park vector includes all the information that is displayed in the three currents i_a, i_b, and i_c of the three-phase system. Therefore, the Park vector spectrums for the healthy engine case and the degraded engine were obtained.

Figure 6 illustrates these spectrums of the current i_d and i_q Park vector, and the results of the frequencies characterizing the unbalance defect are given in Table 2.

Table 2. Predictions of the mass unbalance by stator current multiple approaches.

Current induction motor	Frequency (Hz)		Amplitude (dB)	
	$f_{unb\,\max}$	$f_{unb\,\min}$	$A_{unb\,\max}$	$A_{unb\,\min}$
i_a	73.24	26.37	–2.901	–2.999
i_b	73.24	26.37	–3.065	–3.202
i_c	72.27	27.34	–3.113	–3.193
i_d	73.24	25.39	–2.791	–3.020
i_q	72.27	25.39	–2.760	–3.048

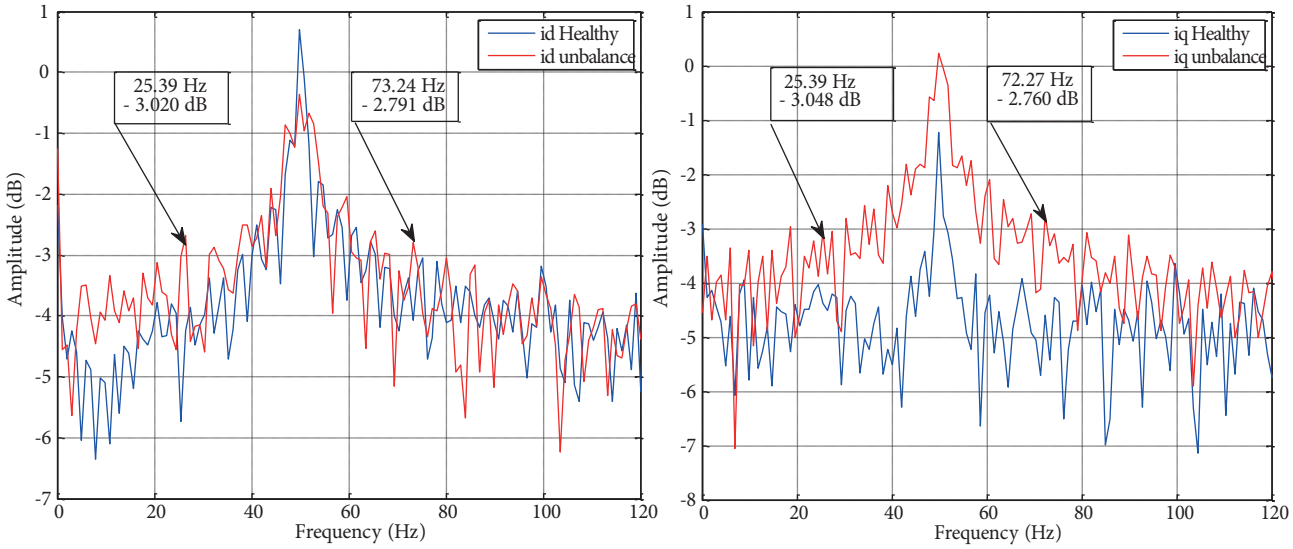

Figure 6. Spectrum of the current i_d and i_q Park vector, healthy and degraded motor.

5.4. Application of STFT to the Park vector of stator current

The spectrogram of Figure 7a shows the case of the healthy motor. We note in bright red color the fundamental harmonic and the fifth harmonic. Figure 7b shows the case of the engine in the presence of the unbalance, where we can note the increase in the signal density of the fundamental harmonic and the fifth harmonic as well as the emergence of peaks at frequencies ($f_s \pm f_r$), validating the presence of the unbalance defect.

5.5. Organizational detection and diagnosis of the fault unbalance

The diagram in Figure 8 provides an overview of the methodology used for the diagnosis of a mechanical degradation and the sequence of analytical approaches of the stator current we performed in order to first signal the presence of any anomaly affecting the system and then to identify the nature of the degradation. Thus, if we first observe a deformation of the orbit in relation to the healthy case, this means that there is a defect. A spectral analysis (FFT and STFT) is then performed. If we observe an increase in harmonic peaks at the characteristic frequencies $f_s \pm (1 \times f_r)$ compared to the healthy case, then there is the presence of an unbalance. In this case, it is necessary to program a maintenance to correct this unbalance via balancing, which will be applied when the engine is stopped. For future research perspectives, we plan to conduct several

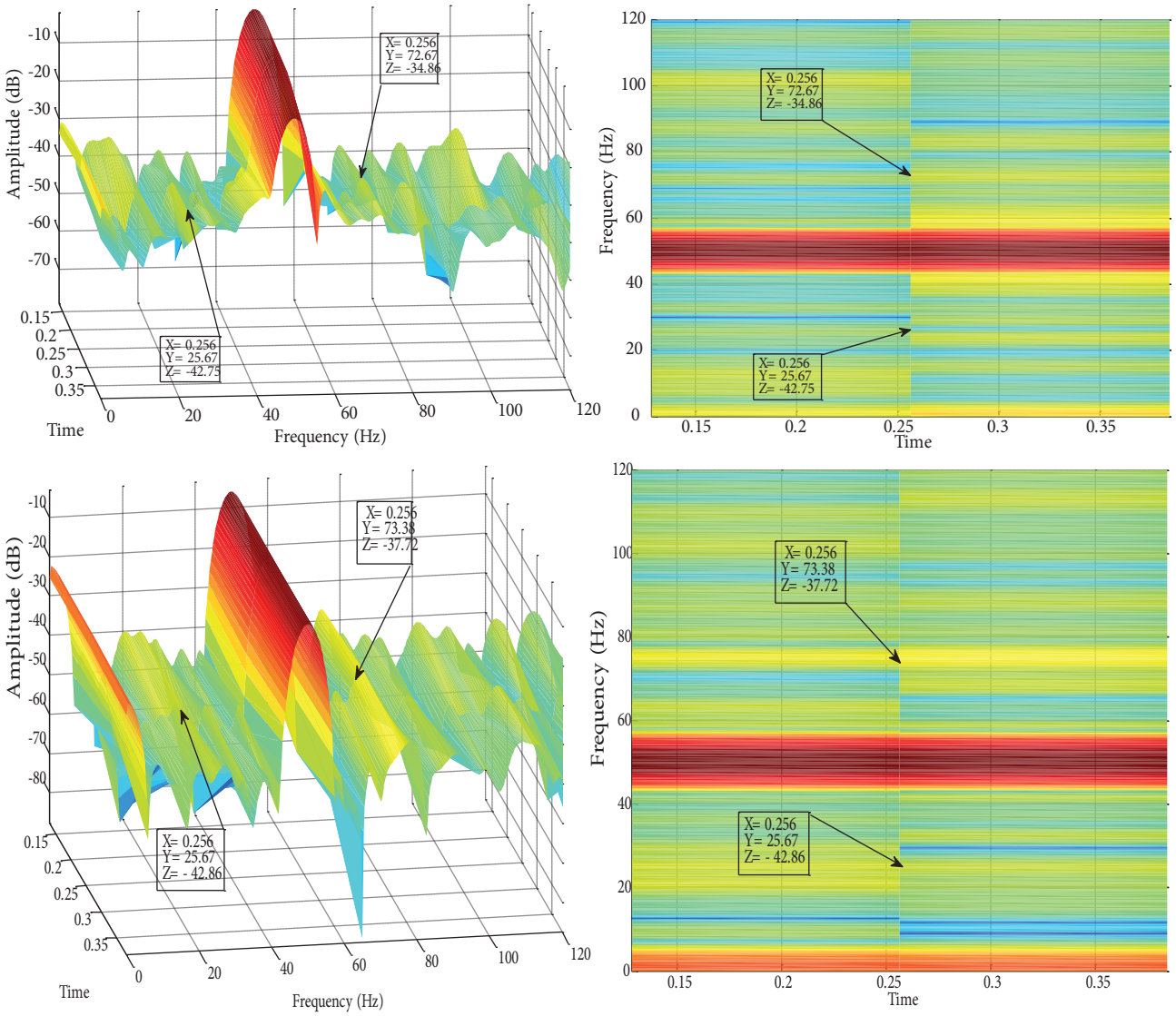

Figure 7. a) Application of STFT to the Park vector of stator current, healthy motor: 3D and orthogonal view. b) Application of STFT to the Park vector of stator current, degraded motor: 3D and orthogonal view.

experiments on our test bench, which will consist of adding other combined defects (mechanical and electrical) and then carrying out a comparative spectral analysis before and after performing corrective maintenance.

6. Experimental implementation of the impact of the unbalance defect during the speed variation of the motor

In order to experimentally study the impact of an unbalance defect when the engine is operating at different speeds and by varying frequencies from 50 Hz to 35 Hz and then to 25 Hz, the FFT approach is applied to the Park vector for the case of the healthy engine and that of the degraded engine. We obtain the spectrum of the Park vector and note a remarkable increase in the amplitudes of the components of the current vector in the case of the degraded engine as soon as the speed is reduced.

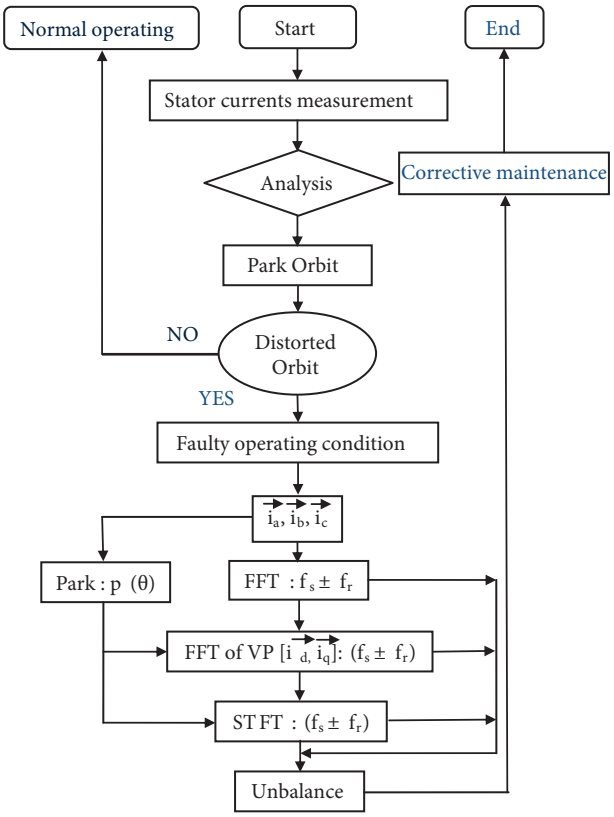

Figure 8. Chart of the sequence of diagnostic approaches unbalance.

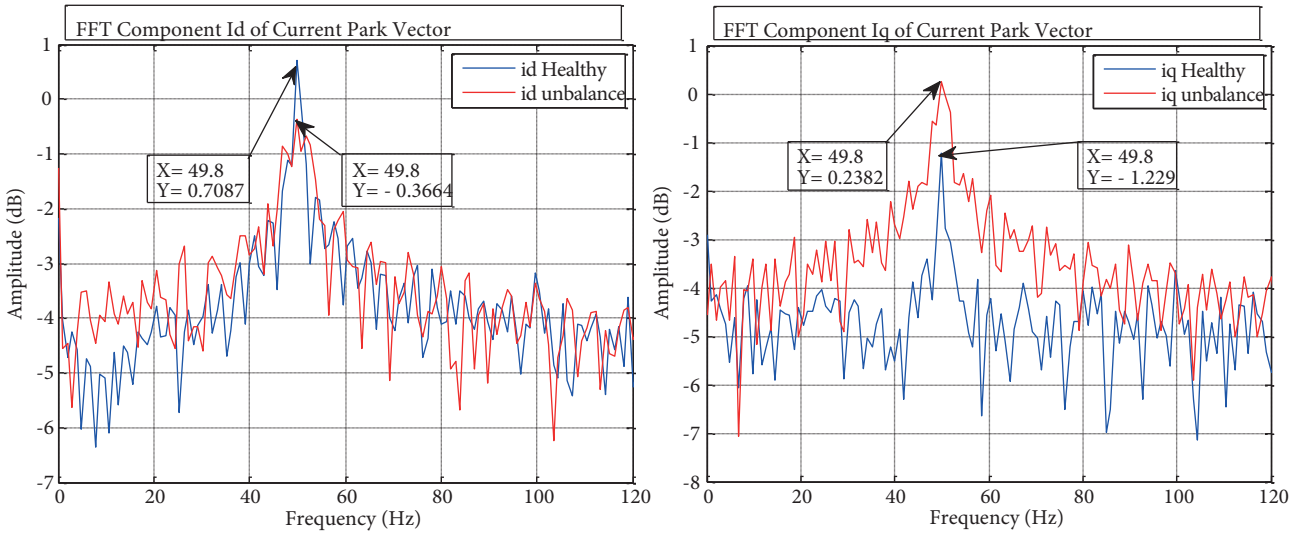

Figure 9. Spectrum of the current i_d and i_q in 1470 rpm, healthy and degraded motor.

We note that the amplitude of the direct component i_d at a speed of 1470 rpm is –0.3664 dB (Figure 9), while in Figure 10, where the speed decreases to 1050 rpm, the amplitude of the component i_d is 0.5910 dB, and for a speed of 735 rpm the amplitude is 0.5260 dB (Figure 11). Table 3 summarizes the results expressed by the characteristic frequencies and their amplitudes. The unbalance generates a vibration with an amplitude

that can vary greatly according to the speed of rotation, and that the severity of the mass unbalance is inversely proportional to the speed variation, which implies a worsening of the defect.

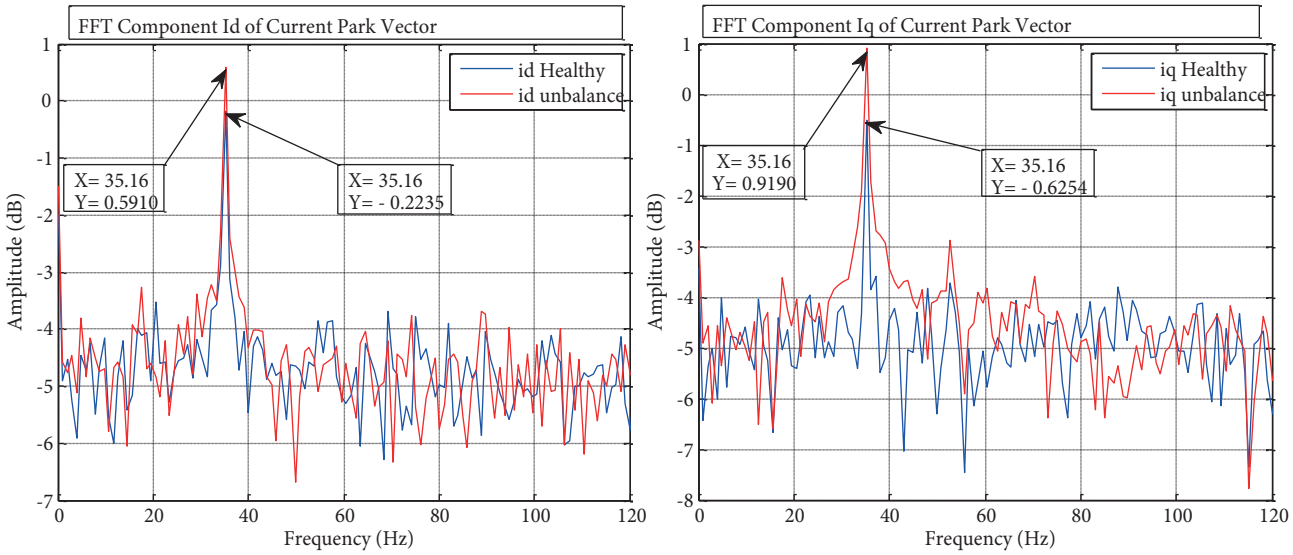

Figure 10. Spectrum of the current i_d and i_q in 1050 rpm, healthy and degraded motor.

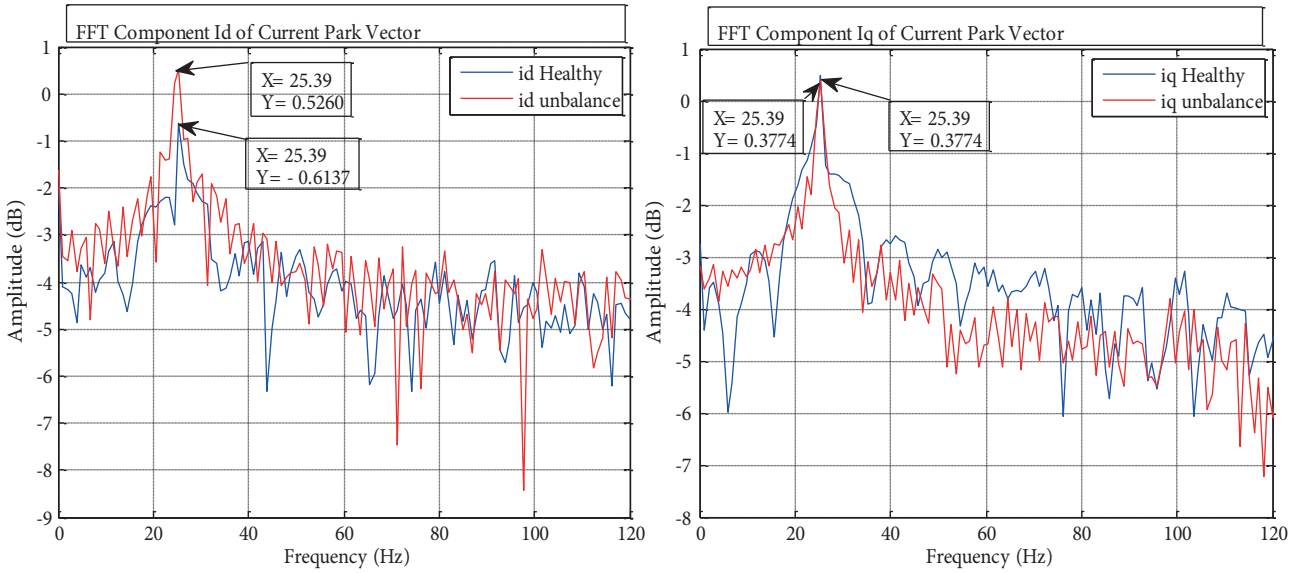

Figure 11. Spectrum of the current i_d and i_q in 735 rpm, healthy and degraded motor.

7. Conclusion

The unbalance defect targeted in this experimental work has been identified on an asynchronous motor of 270 W. The results obtained through this technique using a sequence of approaches of the stator current were very conclusive. This multiple technique has involved the Park orbit to indicate a dysfunction of the electrical drive, supplemented by current Fourier transforms (MCSA, EPVA, STFT) to help identify the type of degradation.

Table 3. Fault severity with speed variation.

Speed induction motor at no load		Current i_d		Current i_q	
		Frequency (Hz)	Amplitude (dB)	Frequency (Hz)	Amplitude (dB)
1470 rpm (50 Hz)	Healthy	49.80	0.7087	49.80	–1.2290
	Unbalance	49.80	–0.3664	49.80	0.2382
1050 rpm (35 Hz)	Healthy	35.16	–0.2235	35.16	–0.6254
	Unbalance	35.16	0.5910	35.16	0.9190
735 rpm (25 Hz)	Healthy	25.39	–0.6137	25.39	0.3774
	Unbalance	25.39	0.5260	25.39	0.3774

A diagram has been produced to illustrate the application of this methodology adapted to the detection and diagnosis of the unbalance defect. Since the operation of the induction motor is becoming more widespread in technological processes requiring variable speed, a severity curve indicating the severity of the unbalance defect under this mode of operation is provided at the end of this study.

This methodology can be transposed to the diagnosis and predictive detection of other types of failures affecting electrical drives that have a variable speed induction motor.

References

[1] Li W, Mechefske CK. Detection of induction motor faults: a comparison of stator current, vibration and acoustic methods. J Vib Control 2006; 12: 165-188.

[2] Kia SH, Henao H, Capolino GA. A comparative study of acoustic, vibration and stator current signatures for gear tooth fault diagnosis. In: ICEM 2012 International Conference on Electrical Machines; 2–5 September 2012; Marseille, France: ICEM. pp. 1512-1517.

[3] Iorgulescu M, Beloiu R. Faults diagnosis for electrical machines based on analysis of motor current. In: OPTIM 2014 International Conference on Optimization of Electrical and Electronic Equipment; 22–24 May 2014; Bran, Romania: OPTIM. pp. 291-297.

[4] Blödt M, Granjon P, Raison B, Regnier J. Mechanical fault detection in induction motor drives through stator current monitoring - Theory and application examples. In: Zhang W, editor. Fault Detection. Rijeka, Croatia: INTECH, 2010. pp. 451-488.

[5] Choi S, Pazouki E, Baek J, Bahrami HR. Iterative condition monitoring and fault diagnosis scheme of electric motor for harsh industrial application. IEEE T Ind Electron 2015; 62: 1760-1769.

[6] Salah M, Bacha K, Chaari A. Stator current analysis of a squirrel cage motor running under mechanical unbalance condition. In: IEEE 2013 10th International Multi-Conference on Systems, Signals & Devices (SSD); 18–21 March 2013; Hammamet, Tunisia: IEEE. pp. 1-6.

[7] Granjon P, Vieira M, Sieg-Zieba S. Surveillance du désalignement d'un moteur asynchrone par analyse du vecteur d'espace courant. In: Workshop of GIS 2009 Surveillance, sureté, sécurité des grands systèmes; 3–4 June 2009; Nancy, France: GIS. pp. 1-7.

[8] Zarei J, Poshtan J. An advanced park's vectors approach for bearing fault detection. In: IEEE 2006 Conference on Industrial Technology; 15–17 December 2006; Mumbai, India: IEEE. pp. 1472-1479.

[9] Fernao Pires AV, Martins JF, Pires AJ. Eigenvector/eigenvalue analysis of a 3D current referential fault detection and diagnosis of an induction motor. Energ Convers Manage 2010; 51: 901-907.

[10] Obaid RR, Habetler TG. Effect of load on detecting mechanical faults in small induction motors. In: SDEMPEDS 2003 Symposium on Diagnostics for Electric Machines, Power Electronics and Driver; 24–26 August 2003; Atlanta, GA, USA: IEEE. pp. 307-311.

[11] Intesar A, Manzar A, Kashif I, Shuja Khan M, Junaid Akhtar S. Detection of eccentricity faults in machine using frequency spectrum technique. International Journal of Computer and Electrical Engineering 2011; 3: 111-119.

[12] Blödt M, Chabert M, Regnier J, Faucher J. Mechanical load fault detection in induction motors by stator current time-frequency analysis. IEEE T Ind Appl 2006; 42: 1454-1463.

[13] Metatla A, Benzahioul S, Bahi T, Lefebvre D. On line current monitoring and application of a residual method for eccentricity fault detection. Adv Electr Comput En 2011; 11: 69-72.

[14] Fernández Gómez AJ, Sobczyk TJ. Motor current signature analysis apply for external mechanical fault and cage asymmetry in induction motors. In: SDEMPED 2013 9th IEEE International Symposium; 27–30 August 2013; Valencia, Spain: IEEE. pp. 136-141.

[15] Krishna MSR, Ravi KS. Fault diagnosis of induction motor using motor current signature analysis. In: ICCPCT 2013 International conference on circuits, power and computing technologies; 20–21 March 2013; Nagercoil, India: IEEE. pp. 180-186.

[16] Leite VCMN, Borges da Silva JG, Cintra Veloso GF, Borges da Silva LE. Detection of localized bearing faults in induction machines by spectral kurtosis and envelope analysis of stator current. IEEE T Ind Electron 2015; 62: 1855-1865.

[17] Messaoudi M, Sbita L. Multiple faults diagnosis in induction motor using the MCSA method. International Journal of Signal and Image Processing 2010; 1: 190-195.

[18] Pires VF, Kadivonga M, Martins JF, Pires AJ. Motor square current signature analysis for induction motor rotor diagnosis. Elsevier Measurement 2013; 46: 942-948.

[19] Martins JF, Pires VF, Amaral T. Induction motor fault detection and diagnosis using a current state space pattern recognition. Pattern Recogn Lett 2011; 32: 321-328.

[20] Sonje DM, Chowdhury A, Kundu P. Fault diagnosis of induction motor using parks vector approach. In: ICAEE 2014 International Conference on Advances in Electrical Engineering; 9–11 January 2014; Vellore, India: IEEE. pp. 1-4.

[21] Diallo D, Benbouzid MEH, Hamad D, Pierre X. Fault detection and diagnosis in induction machine drive: a pattern recognition approach based on Concordia stator mean current vector. IEEE T Energy Conver 2005; 20: 512-519.

[22] Vieira M, Theys C, Benbouzid MEH. Induction motors faults detection and localisation using stator current advanced signal processing techniques. IEEE T Power Electr 1999; 14: 14-22.

[23] Cruz SMA, Cardoso AZJM. Stator winding fault diagnosis in three phase synchronous and asynchronous motors, by the extended Park's vector approach. IEEE T Ind Appl 2001; 37: 1227-1233.

[24] Flandrin P. Temps – Fréquence. Traité des nouvelles technologies. Paris, France: Edition Hermès, 1993.

[25] Jianguo J, Zhiping Z, Pengshang S, Xiangheng W. Time frequency spectrum (TSF) of line current during starting process – A tool for diagnosing failure of induction motor. In: The International Conference on Electrical Machines; 15–17 September 1992; Manchester, United Kingdom: ICEM. pp. 1261-1265.

[26] Cohen L. Time Frequency Analysis. Upper Saddle River, NJ, USA: Prentice Hall, 1995.